



Effect of double ageing on performance and establishment of prediction model for 6005 aluminum alloy

WANG Xu-cheng(王旭成)^{1,2}, HUANG Yuan-chun(黄元春)^{1,2*}, ZHANG Li-hua(张立华)²,
ZHANG Yun(张昀)², HUANG Shi-ta(黄仕塔)³

1. State Key Laboratory of High Performance Complex Manufacturing, Central South University, Changsha 410083, China;

2. College of Mechanical and Electrical Engineering, Central South University, Changsha 410083, China;

3. Antai New Energy Technology Co., Ltd., Zhangzhou 363000, China

© Central South University 2022

Abstract: In the present investigation, the relation of pre-ageing temperature and pre-ageing time to mechanical properties was studied, and a model was established to predict the mechanical properties of AA6005 Al alloy. Compared with the experimental results, the deviation of the proposed model was limited to 8.1%, which showed reasonable accuracy of forecasting. It was found that the performance of AA6005 alloy was better at higher pre-ageing temperature with shorter pre-ageing time than that at T6 temper. The microstructure of the alloy was observed by transmission electron microscopy, and the results showed that high dislocation density and precipitate density existed at 160 °C and 200 °C pre-ageing, which were in good agreement with the model.

Key words: Al alloy; heat treatment; model; mechanical performance; strengthening mechanism

Cite this article as: WANG Xu-cheng, HUANG Yuan-chun, ZHANG Li-hua, ZHANG Yun, HUANG Shi-ta. Effect of double ageing on performance and establishment of prediction model for 6005 aluminum alloy [J]. Journal of Central South University, 2022, 29(3): 973–985. DOI: <https://doi.org/10.1007/s11771-022-4976-y>.

1 Introduction

In transportation and aircraft industry, it is important to reduce the product weight because of energy saving [1, 2]. These requirements have motivated the materials design violently in past decades. In traditional materials, ceramic materials are liable to brittle fracture, polymer materials are unstable at high temperature, they both cannot adapt to the complicated and changeable environment in aerospace and transportation due to unalterable

disadvantages, while the advantages of metal materials are highlighted. Especially, aluminum alloy is becoming advanced materials in various fields because of the low-weight [3], moderate strength [4] and excellent formability [5], and many experts pay attention to grain refinement, enhancement of dislocation density, precipitation sequence by altering alloy components [3, 4], proceeding severe plastic deformation [5] and optimizing ageing regime [6].

Compared with other aluminum alloys, 6xxx aluminum alloys (Al-Mg-Si(-Cu) alloy) possess

Foundation item: Projects(51575539, U1837207) supported by the National Natural Science Foundation of China; Project(2020RC2002) supported by the Science and Technology Innovation Program of Hunan Province, China; Project(2021JJ40774) supported by Natural Science Foundation of Hunan Province, China

Received date: 2021-06-26; **Accepted date:** 2022-01-06

Corresponding author: HUANG Yuan-chun, PhD, Professor; E-mail: ychuang@csu.edu.cn; ORCID: <https://orcid.org/0000-0002-8998-563X>

numerous irreplaceable advantages, such as excellent formability, outstanding corrosion resistance, medium tensile strength, and low manufacturing cost [3], and plenty of works have been done to improve the mechanical properties of aluminum alloys in different conditions. XIA et al [7] designed an innovative RRA treatment to enhance fatigue crack resistance, which indicated that suitable RRA treatment can improve materials performance. Many other researches focus on the corrosion behavior of heat treatment [8, 9], but also obtained great strength and ductility [10, 11]. CHANG et al [12] researched different ageing treatments of AA6060 aluminum alloy, and the results manifested that it can significantly improve the alloy hardness and tensile strength by natural pre-ageing and subsequent high temperature ageing in a short time, the natural ageing can produce a high density of clusters or co-clusters of Si and Mg solute atoms that control the precipitation kinetics of subsequent artificial ageing during which the clusters dissolve slowly and might serve as nucleation sites for subsequent precipitation. ABÚNDEZ et al [13] showed that the ultimate tensile strength (UTS) of 6061 aluminum alloy could be improved by two-step ageing heat treatment, and established a mathematical relationship of alloy including hardness and ultimate tensile strength, pre-ageing temperature was considered to relate to UTS and hardness.

It is well known that 6xxx aluminum alloy can be strengthened by heat treatment, and precipitation strengthening is an important mechanism to improve the mechanical properties significantly, it has attracted many experts for several decades to explore the effects of pre-treatment during ageing treatment. ENGLER et al [14] studied the effect of natural ageing and pre-ageing on the evolution of precipitate structure and strength of Al-Mg-Si alloy AA6016, the results demonstrated that pre-ageing heat treatment is beneficial to the nucleation of β'' phase, and reduced insoluble clusters of Mg and Si atoms. YIN et al [15] studied the effects of pre-straining on the hardening behavior during ageing heat treatment of Al-Mg-Si-Cu alloy, the results indicated that pre-straining significantly increased the peak ageing hardness and shortened the peak ageing time of the alloy. Moreover, it restrained the formation of clusters/GP zones and accelerated the

nucleation of β'' and Q' phases in the early stage of subsequent artificial ageing, significantly decreased the negative effects of natural ageing on the hardening behavior of the alloy during subsequent artificial. JIN et al [16] studied pre-ageing and pre-straining uniformly, the result showed that pre-treatment suppressed the negative effect of natural aging completely, and the pre-treatment can generate the β -nuclei to be readily transformed into β'' phase during artificial ageing. GONG et al [17] designed a high-performance Al-Mg-Si-Cu-Zn alloy, and achieved high bake hardening response via optimized pre-ageing treatments.

The researches of pre-ageing treatment were mainly existed in 6111 [17], 6016 [17, 18] and 6022 [19] Al alloys, however, the effects of pre-ageing treatment on 6005 Al alloys have been ambiguous, the interaction between pre-ageing time and pre-ageing temperature of 6005 Al alloy have been ignored so far, and the relation between pre-ageing temperature and pre-ageing time has not been established. In this work, the effects of pre-ageing temperature and pre-ageing time on hardness and UTS have been studied. In order to further improve the performance of 6005 Al alloy and explore suitable heat treatment for future application, an optimized model including the nonlinearity interactions was established based on two factors (pre-ageing temperature and pre-ageing time) to relate with hardness and UTS. Meanwhile, microstructure characterization and strengthening mechanism provided comprehensive explanations to evaluate the microstructure-property relationships in this alloy.

2 Experimental

Commercial extruded 6005 aluminum alloy of 2.0 mm in thickness was used in the present work. The chemical composition of the alloy is: 0.2% max Si, 0.1% max Cu, 0.35% max Fe, 0.4% max Mg, 0.1% max Mn, 0.1% max Cr, 0.25% max Zn, 0.1% max Ti and balance Al. Mechanical properties after T6 heat treatment (ageing at 180 °C for 6 h) were: 223 MPa yield strength (YS), 262 MPa ultimate tensile strength (UTS), as received condition.

Solution treatment and ageing treatment were both carried out in samples. The solution treatment was carried out at 540 °C for 1 h and quenched in

water subsequently, the ageing treatment was divided into two steps: the first step was termed as pre-ageing, four kinds of pre-ageing temperatures and four kinds of pre-ageing time were selected for the pre-ageing treatment; the second step was termed as ageing, each sample was aged at 180 °C for 6 h. The pre-ageing treatment and ageing treatment were conducted in a heat treatment furnace without any special conditions. A schematic of the heat treatment procedure is shown in Figure 1. The samples were numbered in the form of letter+number, A – E represented different pre-ageing time of 15, 30, 45, 60, 75 min, respectively, 1 – 4 represented different pre-ageing temperature of 140 °C, 160 °C, 200 °C, 220 °C, respectively. For example, C3 represented the sample was pre-aged at 200 °C for 45 min, and E4 represented the sample was preaged at 220 °C for 75 min.

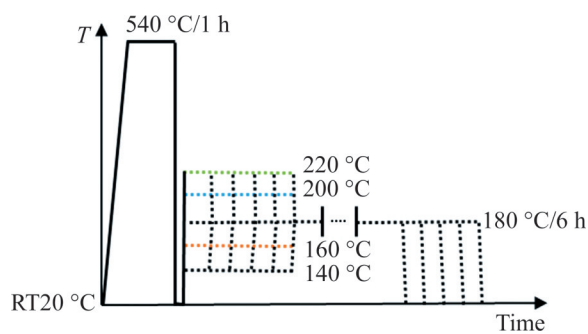


Figure 1 Pre-ageing and ageing treatment for selected temperatures

The hardness was measured by HuaYin HV-1000A Vickers hardness tester with a load of 100 g and a dwell time of 30 s, five indentations were made in each sample to obtain a reliable average hardness value. Tensile specimens were prepared in accordance with ASTM E8, with a thickness of 2 mm, and the testing machine was INSTRON 3400, the employed test rate was 2 mm/min. Microstructural observations were carried out in Olympus DSX1000 optical microscope, VEGA3 XMU scanning electron microscope and Tecnai G20 transmission electron microscope. Thin foils for TEM experiments were prepared by further cutting and grinding down to disks with thickness of about 30 μm, and then punching them into some φ3 mm disks. Twin-jet polishing was further carried out in the 10% perchloric acid ethanol solution electrolyte at -35 °C. The operating voltage of TEM was kept at 200 kV.

3 Results and discussion

3.1 Hardness

Table 1 shows the hardness data for each heat treatment process, each heat treatment process corresponds to a hardness value, so the hardness value(HV) can therefore be regarded as a binary function of pre-ageing time and pre-ageing temperature as independent variables, i.e., $HV=f(\text{time, temperature})$. Considering the nonlinear effects of temperature and time on hardness, these data were studied by multiple nonlinear regression method to establish a polynomial equation that correlates HV with pre-ageing time (t_r) and pre-ageing temperature (T_r) showed as Eq. (1).

$$HV = a_0 + a_1 t_r + a_2 T_r + \dots + a_q t_r^m T_r^n \quad (1)$$

where $a_0+a_1t_r+a_2T_r$ represents the typical linear factor of the model; different exponents of t_r and T_r represent the varying degrees of interaction effect; a is the influence coefficient. In a previous study, a polynomial equation with respect to treatment parameters of 6061 aluminum alloy was established [13]. However, it took only single factor into consideration, and the R -square coefficient was only 0.88. Moreover, the nonlinear interaction effects of

Table 1 Hardness after pre-ageing treatment and 6 h ageing treatment with different heating temperatures and times

Time/min	Hardness (HV)			
	140 °C	160 °C	200 °C	220 °C
15	89.75	99.70	99.37	76.73
30	92.47	98.91	101.93	76.52
45	91.60	95.70	100.77	81.13
60	86.33	96.35	96.03	73.67
75	84.31	98.83	91.62	73.43

time and temperature were ignored. The R -square coefficient depends on the fitting condition, that is, whether the model can accurately calculate the true hardness, the value is closer to 1 when the model is more accurate. Hence two main factors (i.e., pre-ageing temperature and pre-ageing time) were considered into the polynomial function in this study, and the nonlinearity between the pre-ageing time and pre-ageing temperature (i.e. different exponent) was also included. The polynomial

function was showed as Eq. (2), where p represents the coefficient of different interaction effects between pre-ageing time and pre-ageing temperature. The R -square reflects the fluctuation of HV that can be described by the fluctuation of t_r and T_r . The calculation process of R -square is given by Eqs. (3)–(5), where \bar{y} represents the average value of the data in Table 1, y_i represents each data in Table 1. HV_i represents the result of Eq. (2). SS_{tot} represents total sum of squares. SS_{res} represents error sum of squares. The results manifested that the R -square coefficient achieved 0.96, as showed in Table 2, which indicated the accuracy of this optimized model was more reliable.

$$HV(t_r, T_r) = p_{00} + p_{10}t_r + p_{01}T_r + p_{20}t_r^2 + p_{11}t_rT_r + p_{02}T_r^2 + p_{30}t_r^3 + p_{21}t_r^2T_r + p_{12}t_rT_r^2 + p_{03}T_r^3 \tag{2}$$

$$\bar{y} = \frac{1}{20} \sum_i^{20} y_i \tag{3}$$

$$SS_{tot} = \sum_i^{20} (y_i - \bar{y})^2 \tag{4}$$

$$SS_{res} = \sum_i^{20} (y_i - HV_i)^2 \tag{5}$$

$$R^2 = 1 - \frac{SS_{res}}{SS_{tot}} \tag{6}$$

Table 2 Coefficient values and the R -square coefficient for HV correlation

R -square	p_{00}	p_{10}	p_{01}	p_{20}	p_{11}
0.9601	457.3	0.0206	-8.287	-0.0026	-0.0021
	p_{02}	p_{30}	p_{21}	p_{12}	p_{03}
	0.05869	1.353×10^{-5}	-9.69×10^{-6}	-1.069×10^{-6}	1.32×10^{-4}

As can be seen in Figure 2(a), it was obvious that the hardness value of the alloy first increased with the increase of pre-ageing temperature, the peak value achieved HV 101.93 (it increased by 12.3% compared with T6), and decreased subsequently. With the extension of time, the hardness value of the alloy also appeared a similar regular. Especially at 200 °C, the hardness of the alloy was always at a high level from 15 to 60 min, and obtained the maximum at 200 °C for 30 min. Nevertheless, it was maximum in five different heat treatment regimens rather than the maximum in actual heat treatment. Hence an optimization method called Fminsearch Method was employed to

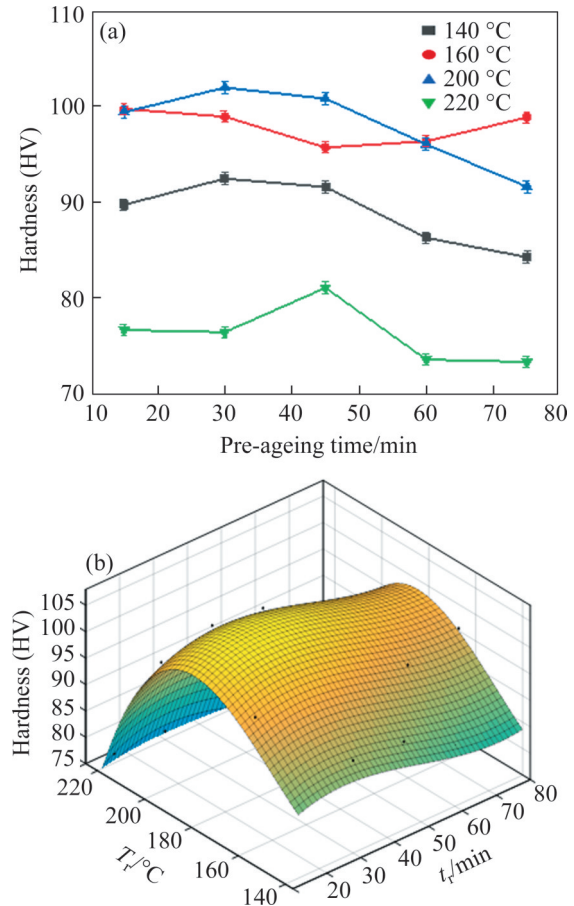


Figure 2 Hardness behavior due to pre-ageing and ageing treatment (a) and multiple prediction model for HV including T_r and t_r (b)

calculate the maximum according to Eq. (2). The results showed the hardness value reached its maximum HV 103.81 when pre-ageing temperature and time were 188.33 °C and 31.74 min, respectively. Compared with the experimental data, the deviations of pre-ageing temperature, pre-ageing time, and hardness were merely 5.8%, 5.8% and 1.8%, respectively. The experiment and prediction values both showed that the heat treatment regime of higher pre-ageing temperature and less pre-ageing time achieve a greater hardness compared to other conditions, which partly agreed with several researches [20, 21]. The reason for this phenomenon can be explained that the strengthening phase is prone to rapid nucleation at high temperature than that in lower temperature due to Fick law. It was obvious that the hardness values of alloy increased first and then decreased at 140, 200 and 220 °C, but the tendency was opposite at 160 °C. This is because 160 °C was slightly lower than 180 °C, and pre-ageing process was equivalent to the early stage

of underage. The effect of recrystallization softening was larger than the effect of precipitation strengthening at first, and achieved balance at 45 min, after which precipitation strengthening played a dominant role. Therefore, the hardness value decreased first and then increased. The precipitation and transformation into metastable state β'' phase and stable β phase in the subsequent process can occur simply because of high difference in concentration. The moderate pre-ageing time was easier to retard β phase growing and coarsening.

3.2 Ultimate tensile strength

The data of UTS were used by multiple nonlinear regression method to find polynomial equation that correlates UTS with two heat treatment parameters (i. e. T_r and t_r) showed as Eq. (1). Specimens were compared to T6 temper (i. e., 262 MPa of UTS and 223 MPa of YS). The test results were showed in Table 3, and the results were plotted in Figure 3(a), which indicated the UTS improved initially and decreased afterward at 140, 160 and 200 °C as pre-ageing temperature increases, the UTS achieved peak (308 MPa) at the pre-ageing temperature of 160 °C for 45 min, which enhanced about 17.6% compared with T6. Meanwhile, the UTS increased most rapidly at 200 °C as pre-ageing time started from 15 to 60 min, and reached the peak value at 60 min. When pre-ageing temperature achieved 220 °C, the UTS value kept dropping. There appeared a distinct phenomenon: the maximum of UTS appeared in a later time as temperature increased, and UTS values have fluctuated significantly and gradually. The reason can be explained that the precipitates can only precipitate adequately and rapidly at high temperature during a long period, so it resulted in larger gap of UTS, while the clusters precipitated

Table 3 UTS after pre-ageing treatment and 6 h ageing treatment with different heating temperatures and time

Time/min	UTS/MPa			
	140 °C	160 °C	200 °C	220 °C
15	262	276	201	275
30	272	295	232	247
45	267	308	283	237
60	257	307	288	223
75	250	271	257	175

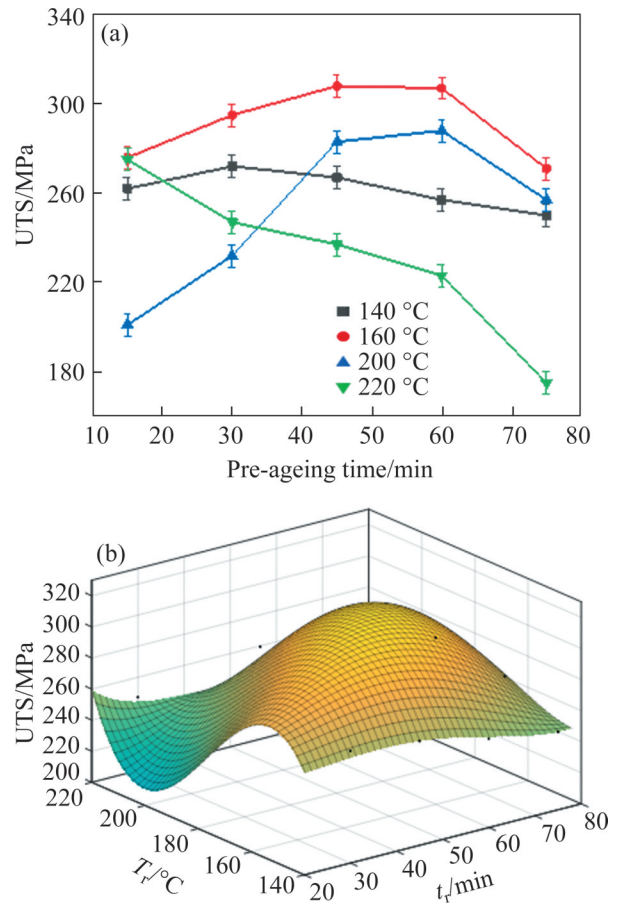


Figure 3 UTS behavior due to pre-ageing and ageing treatment (a) and multiple prediction model for UTS including T_r and t_r (b)

insufficiently at a lower temperature. When the pre-ageing temperature reached 220 °C, UTS kept going down over time, and it indicated that the precipitates precipitated in a short time and began to coarsen at this temperature. This phenomenon illustrated that a lower level of pre-ageing temperature can improve mechanical properties and the results are partly consistent with some literatures [22, 23]. It was noteworthy that the performance of alloy was more stable at low pre-ageing time, and unstable with pre-ageing time increase, especially when pre-ageing time achieved 75 min, the gap of UTS between 160 and 220 °C was 96 MPa, it manifested that a shorter pre-ageing time is more suitable for this alloy. Many previous studies [22, 24, 25] showed that mechanical properties enhanced at higher pre-ageing temperature.

Considering different interactive effects of pre-ageing time and pre-ageing temperature on UTS, a polynomial function showed in Eq. (7) was

employed, and Fminsearch Method was still employed to find optimum solution. It indicated that the maximum of UTS achieved 314.5 MPa at pre-ageing temperature of 173.1 °C for pre-ageing time of 43.7 min based on Fminsearch Method. Compared with the experimental maximum, the deviations of pre-ageing temperature, pre-ageing time and UTS were only 1.9%, 8.1% and 2.9%, respectively, *R*-square coefficient attained 0.9908, as shown in Table 4, they confirmed the precision of this model. There was a remarkable phenomenon only when the highest degree of pre-ageing time and pre-ageing temperature achieved 4 and 3, respectively, the fitting effect achieved the best, and the influence coefficients are shown in Table 4. Large exponent represents larger nonlinearity, this suggested that UTS was more sensitive to pre-ageing time. Compared with pre-ageing temperature, pre-ageing time should be more accurate for high UTS. The different coefficient of *p* represents the coefficient about various interaction effect. It can be observed significantly that high pre-ageing temperature and low pre-ageing time can make alloy achieve higher UTS. This result was partly in agreement with some researches [13, 26]. Meanwhile, high pre-ageing temperature and long pre-ageing time can cause a significant decline of UTS. This phenomenon was observed in some previous literatures [24, 25], which was caused by growth and coarsening of β phase, high pre-ageing temperature and long pre-ageing time will promote precipitate to nucleation, precipitation, and growth, leading to the decrease of UTS.

$$\begin{aligned}
 \text{UTS}(t_r, T_r) = & p_{00} + p_{10}t_r + p_{01}T_r + p_{20}t_r^2 + \\
 & p_{11}t_rT_r + p_{02}T_r^2 + p_{30}T_r^3 + p_{21}t_r^2T_r + p_{12}t_rT_r^2 + \\
 & p_{03}t_r^3 + p_{40}t_r^4 + p_{31}t_r^3T_r + p_{22}t_r^2T_r^2 + p_{13}t_rT_r^3
 \end{aligned}
 \tag{7}$$

3.3 Correlations between hardness, UTS and YS

Hitherto the relation between hardness and UTS of aluminum alloys has still been under

investigation [27, 28]. However, there have been still no straight answers to explain the relation of hardness to UTS under ageing heat treatment. In a previous study [13], author established a relation between hardness and the UTS, regardless of high or low temperature, but a phenomenon has been found that a difference existed between different temperatures in Section 3.1. It can be seen in Figure 4(a) obviously that the UTS values have an uptrend subsequently as hardness increases and can be described as linear relation with HV in the lowest pre-ageing temperature (140 °C). The relationship can be expressed as:

$$\text{UTS} = 2.4\text{HV} + 47 \tag{8}$$

where the value of *R*-square attained is 0.9659, while the correlation between YS and HV has been expressed as [29]:

$$\text{YS} = 3\text{HV} - 48 \tag{9}$$

It indicated that these two empirical formulas were both in accord with experiment data when the sample was subjected to low pre-ageing temperature, while no linear relation emerged in the sample at high pre-ageing temperature as shown in Figure 4(b), and the polynomial fitting curve manifested an inferior value of *R*-square (0.5824). Nevertheless, the UTS increased first and decreased subsequently in the highest pre-ageing temperature (220 °C). UTS values showed more smooth with the increase of hardness partly, while UTS showed strong partial fluctuation. A similar phenomenon emerged in Figure 4(d), which indicated that YS values have the same change with UTS. Therefore, the relation of hardness to UTS/YS can be variable with temperature and should be divided into two parts: high pre-ageing temperature part and low pre-ageing temperature. In a word, there may be no obvious relationship between hardness and UTS/HV. Meanwhile the ASTM has not yet published a standard regarding aluminum hardness and UTS/YS correlations. This may be the reason why there is no

Table 4 Coefficient values and the *R*-square coefficient for UTS correlation

<i>R</i> -square	<i>P</i> ₀₀	<i>P</i> ₁₀	<i>P</i> ₀₁	<i>P</i> ₂₀	<i>P</i> ₁₁	<i>P</i> ₀₂	<i>P</i> ₃₀
0.9908	280.4	129.7	-206.4	-0.597	-2.752	-1.235	-2.468×10 ⁻³
	<i>P</i> ₂₁	<i>P</i> ₁₂	<i>P</i> ₀₃	<i>P</i> ₄₀	<i>P</i> ₃₁	<i>P</i> ₂₂	<i>P</i> ₁₃
	4.877×10 ⁻³	1.82×10 ⁻²	2.43×10 ⁻³	3.56×10 ⁻⁵	2.802×10 ⁻⁵	2.394×10 ⁻⁵	-4.007×10 ⁻⁵

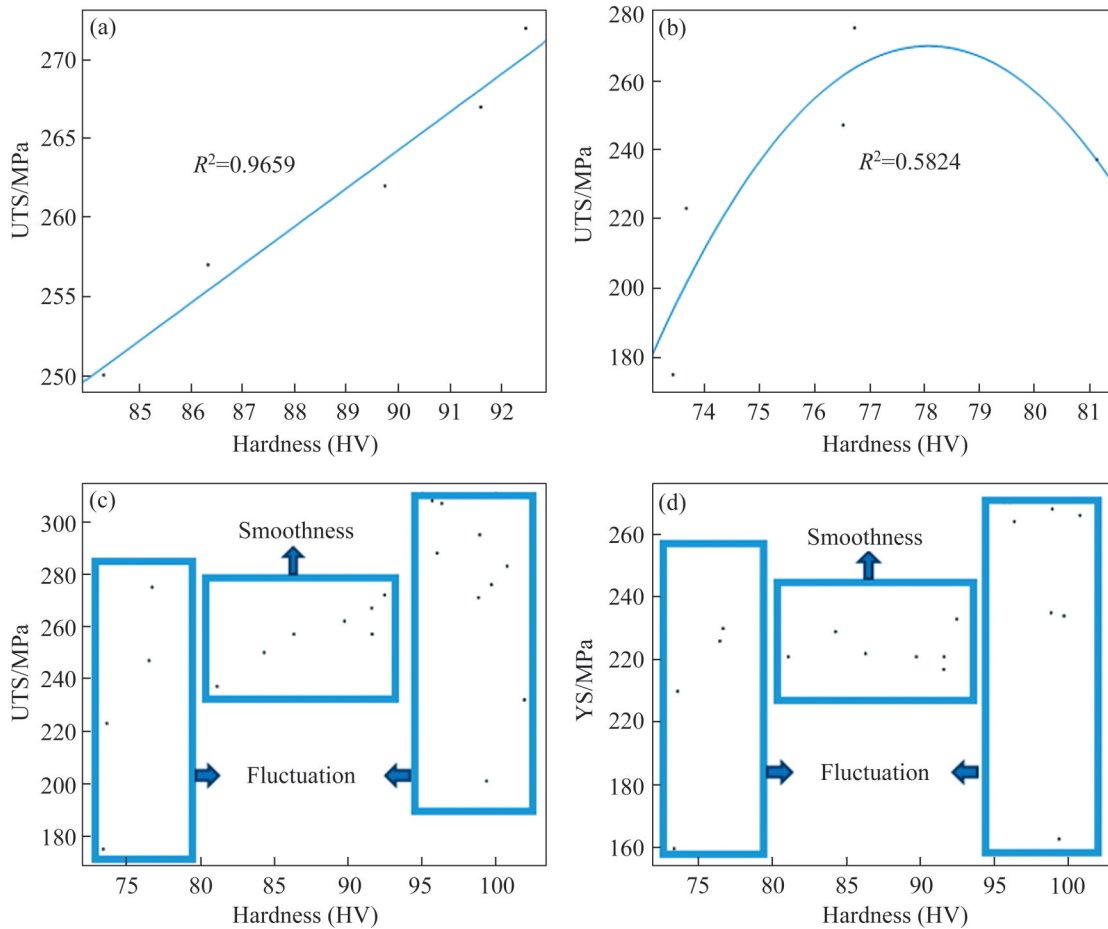


Figure 4 Relation of UTS to hardness at 140 °C pre-ageing + 180 °C ageing treatment (a); Relation of UTS to hardness at 220 °C pre-ageing+180 °C ageing treatment (b); Comparison of experimental data between UTS and hardness (c); Comparison of experimental data between YS and hardness (d)

correlation standard between hardness and UTS [13, 30].

3.4 Microstructural observations

Microstructural features after pre-ageing treatment are shown in Figure 5. Figure 6 shows that an obvious difference existed in grain size and shape due to pre-ageing treatment. A – E mainly exhibited a same tendency about grain evolution (i.e., the grain length decreased with time and temperature increasing). The average grain size reduced from 335 μm in A1 to 257 μm in E1, 301 μm in A2 to 202 μm in E2, 253 μm in A3 to 180 μm in E3 and 193 μm in A4 to 158 μm in E4. The length-diameter ratio of grain appeared the same tendency (i.e., the ratio decreased as time and temperature increase significantly), the average length-diameter ratio reduced from 10.8 in A1 to 6.4 in E1, 8.6 in A2 to 4.5 in E2, 6.3 in A3 to 4.3 in E3 and 5.2 in A4 to 3.8 in E4, there is a clear

phenomenon that: 1) the length-diameter ratio decreased as temperature and time increase and the rate of decrease also reduced as temperature increases; 2) morphology of grains transformed from fibrous size into sphere or ellipse as temperature and time increase. It means that equiaxed grain grow up in pre-ageing stage gradually, and it can improve strength and ductility significantly. These features had also important effects on UTS and YS, and similar features were reported by literature [31]. The diagram evolution of grains can be speculated in Figure 7. With the increase of pre-ageing time, different elements prefer to cluster at the side of grain, resulting in the local concentration enrichment, and tend to separate out from the matrix due to Fick’s law. The fibrous grain gradually bows at the side edge, which includes a high concentration of element atoms (as seen in Figure 5) and separates into two parts. One of them still maintains fibrous structure, much

shorter than before, and repeats the previous steps until the elements concentration and grain size reach the critical point.

Figure 8 shows the TEM bright-field images of different samples after pre-ageing + ageing heat treatment. A highly dense microstructure of intergranular precipitates existed in sample of A1,

with main growth dimension exceeding 200 nm in length, meanwhile, there was a phenomenon which did not appear in other samples, i. e., there were many phases including Mn element existed in matrix (blue arrows) [32], and the shape of these phases approximated sphere or ellipse, with radii ranged from 23 nm to 48 nm. Previous studies

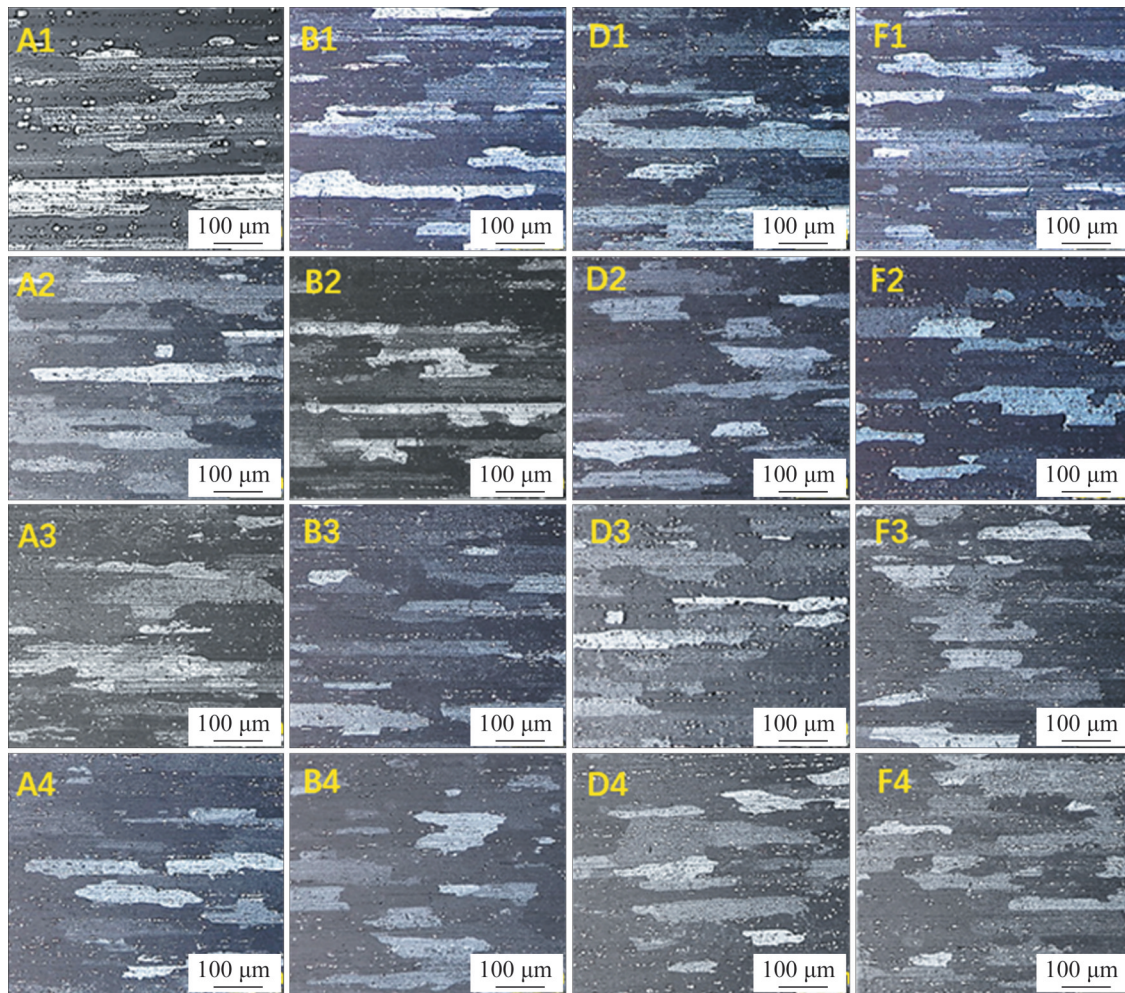


Figure 5 Microstructure in different pre-ageing conditions under optical microscope

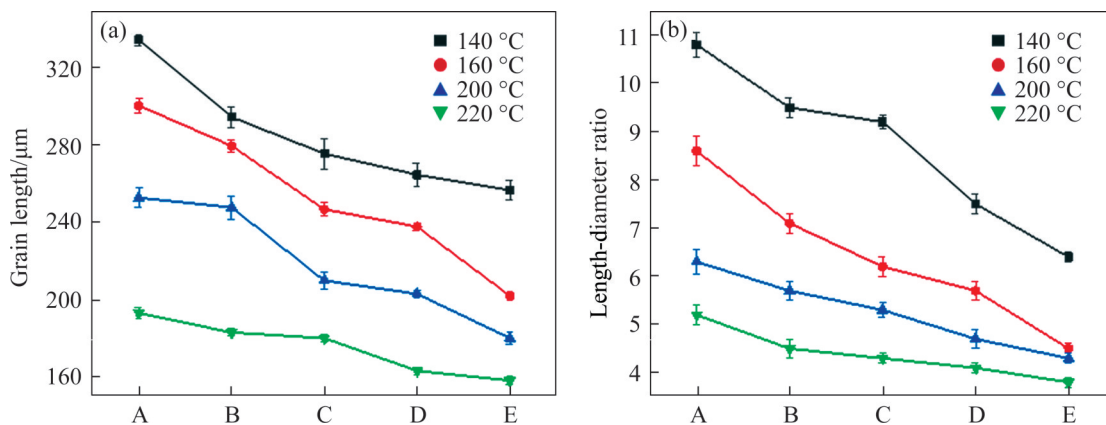


Figure 6 Grain length of samples in different pre-ageing condition (a); Length-diameter ratio of samples in different pre-ageing condition (b)

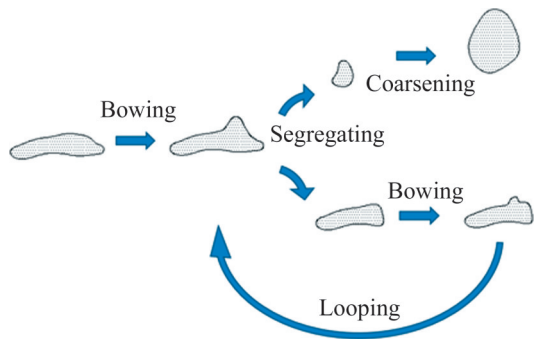


Figure 7 Schematic diagram of grain shape and size evolution

confirmed the addition of Mn element can promote nucleation and result in strength improvement [32, 33]. Compared with A1, E4 existed less dense microstructure of intergranular precipitates, although the size of precipitates had decreased, and the strength of E4 was inferior to A1. Near the peak

ageing temperature, i.e., 200 °C for 45 min (C3) and at 160 °C for 60 min (D2), the microstructures comprised high densities of needle β phase precipitates with characteristic strain contrast running parallel to the main growth direction [34], high dislocation density existed in both two states, and the density of precipitates in D2 was more than that in C3 evidently, this phenomenon was consistent with that the dislocation density existed in D2 was higher than that existed in C3. β'' phase was considered as the main strengthening phase in Al-Mg-Si alloy, it prefers to nucleating near dislocation due to high stored energy resulted from atomic disorder [35], nucleation of β'' phase is in favor of releasing energy and resulting in a steady state according to lowest energy principle. The strength of D2 (307 MPa) was prior to the strength of C3 (288 MPa), this phenomenon demonstrated that the dislocation density and high densities of

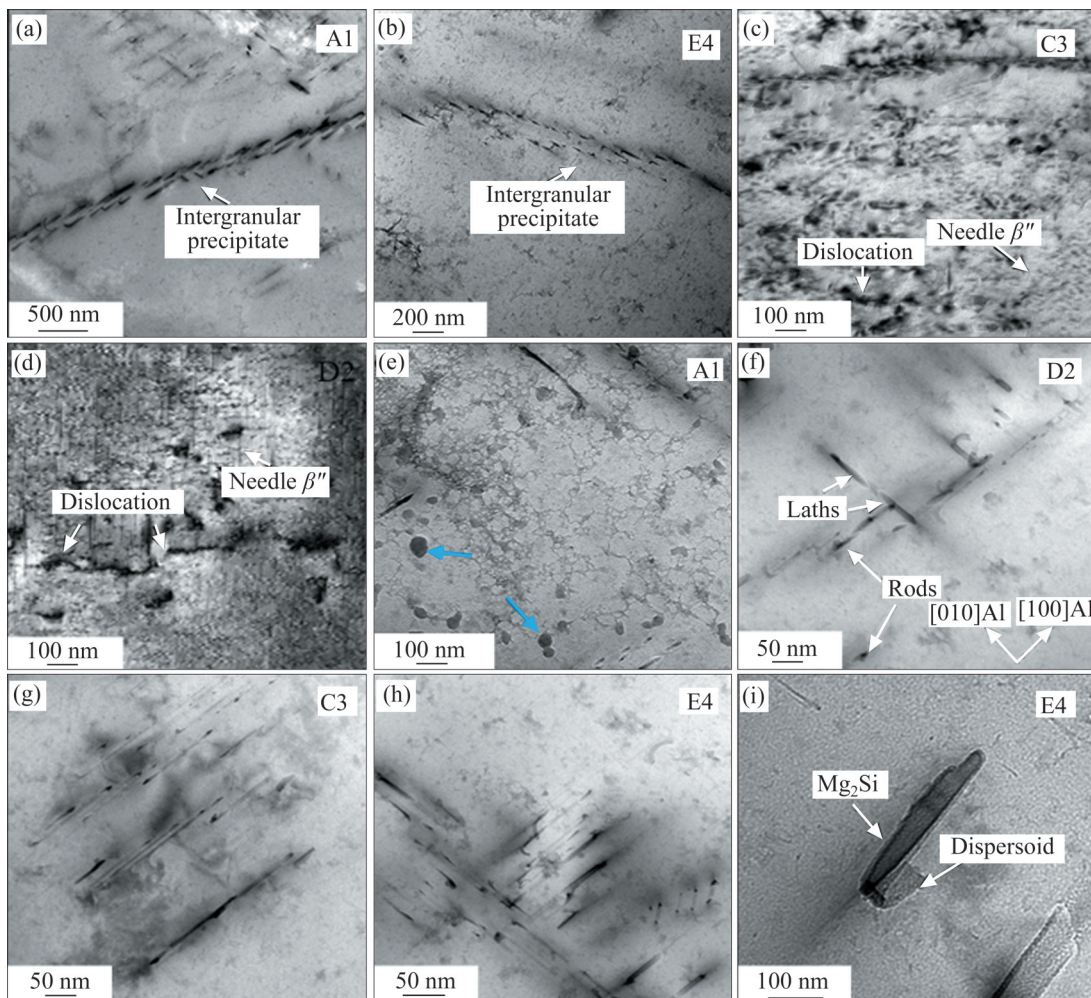


Figure 8 Bright-field TEM images of aged alloys: (a, e) Pre-aged at 140 °C for 15 min+aged at 180 °C for 6 h; (d, f) Pre-aged at 160 °C for 60 min+aged at 180 °C for 6 h; (c, g) Pre-aged at 200 °C for 45 min+aged at 180 °C for 6 h; (b, h, i) Pre-aged at 220 °C for 75 min+aged at 180 °C for 6 h

needle β'' phase precipitates have prominent effects to the performance of alloy. Previous researches manifested that β'' phase is constituted of Mg and Si elements, and the crystal structure is considered as Mg_3Si_6 , [35, 36] which has excellent effects (i. e., precipitation strength and dispersion strength) to hinder dislocation motion to improve performance. The high densities of needle β'' phase improve the strength of alloy due to the pinning effects occurred at dislocation [36]. As the ageing time increases, needle β'' phase began to coarsen gradually, and transformed into stable β phase (Mg_2Si), which could result in the strength decrease.

During ageing treatment, the variation of hardness is primarily related to precipitates transformation in grains. The precipitates tend to nucleate near the dispersive AlFe(Mn)Si phase [37], the predecessor of AlFe(Mn)Si phase is considered as Al5FeSi phase, and the precipitation mechanism of Al5FeSi phase can be described in Figure 9(a) [38]. Nucleation sites of AlFe(Mn)Si phase are liable to locating at the surface of thick AlFeSi phase because this position can achieve critical nucleation concentration due to rapid diffusion of Fe and Si atoms, then diffusion and growth will proceed at the same time controlled by Fick's law. With increasing the ageing time, segregation of solute atoms intensifies, resulting in cutting off the previous phase, and a phenomenon called solution penetration occurs. Solution penetration mechanism is interpreted as the main measure to form fine dispersive phase, and Figure 8(i) shows that β phase (Mg_2Si) existed in E4 attached with phase including Mn element. MYHR et al [39] explained that the resulting expression for the overall macroscopic yield strength σ_y can be expressed as:

$$\sigma_y = \sigma_i + \sigma_{ss} + \sigma_p \quad (10)$$

where σ_i is the intrinsic yield strength of pure aluminium, which is constant close to only 10 MPa [14, 29]; σ_{ss} is the contribution from alloying elements in solid solution to the overall macroscopic yield strength; σ_p is the contribution from hardening precipitates to the overall macroscopic yield strength. σ_{ss} is weakened due to precipitating result in decreasing lattice distortion during ageing treatment. As the ageing time increases, the particles nucleate near AlFe(Mn)Si phase and grow, resulting in the increment of UTS

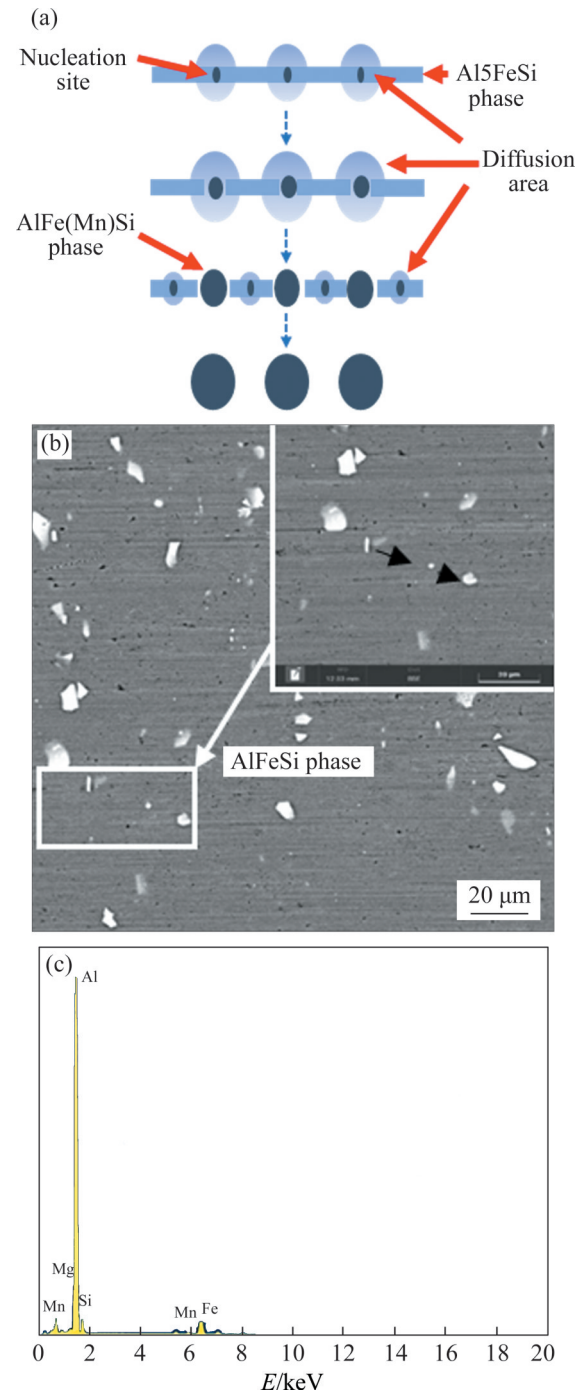


Figure 9 Schematic of model for the nucleation and phase transformation [34] (a), SEM detail of B3 sample (b) and EDS detail of AlFeSi phase (c)

due to the increase of radius of precipitates (Figure 3(a)). However, coarsening process initiates to decrease precipitate density and lattice distortion, while increase particle radius without increase strength [37], and coarsening and reduction of precipitate density will result in the decrease of UTS, YS, and HV as seen from Figures 2(a) and 3(a).

4 Conclusions

In the present investigation, prediction models were established to forecast the mechanical properties of AA6005 Al alloy during double ageing heat treatment, and the microstructures characteristics were analyzed to explain the performance at different double ageing treatments. We concluded the following:

1) Excellent strength and hardness can be achieved during the double ageing treatment. Compared with T6 temper, the maximal hardness of AA6005 Al alloy increased by 12.3% to HV 101.93 at high pre-ageing temperature with short pre-ageing time, and the maximal ultimate tensile strength of AA6005 Al alloy increased by 17.6% to 308 MPa at low pre-ageing temperature with short pre-ageing time.

2) A model was established to predict the mechanical properties of AA6005 Al alloy. Compared with the experimental results, the deviation of the proposed model was limited to 8.1%, which showed reasonable accuracy of forecasting. Meanwhile, the nonlinear effect of pre-ageing time on alloy properties was stronger than that of pre-ageing temperature. There existed an obvious nonlinear relation of hardness to strength at high temperature, hence no typical linear relationship existed between hardness and ultimate tensile strength.

3) The microstructures comprised high dislocation density and high densities of needle β'' phase precipitates with characteristic strain contrast running parallel to the main growth direction during short pre-ageing time, it was connected with the nonlinear effect of pre-ageing time on alloy.

Contributors

HUANG Yuan-chun provided the concept and edited the draft of manuscript. WANG Xu-cheng conducted the literature review and wrote the first draft of the manuscript. ZHANG Li-hua, ZHANG Yun and HUANG Shi-ta analyzed the measured data and edited the draft of manuscript. All authors replied to reviewers' comments and revised the final version.

Conflict of interest

The authors declare that they have no known competing financial interests or personal relationships that could have appeared to influence the work reported in this paper.

Reference

- [1] CHEN Hui-chi, PINKERTON A J, LI Lin, et al. Gap-free fibre laser welding of Zn-coated steel on Al alloy for light-weight automotive applications [J]. *Materials & Design*, 2011, 32(2): 495–504. DOI: 10.1016/j.matdes.2010.08.034.
- [2] CARVALHO U T F, CAMPILHO R D S G. Application of the direct method for cohesive law estimation applied to the strength prediction of double-lap joints [J]. *Theoretical and Applied Fracture Mechanics*, 2016, 85: 140–148. DOI: 10.1016/j.tafmec.2016.08.018.
- [3] CHEN Cun-guang, HAN Wei-hao, QI Miao, et al. Microstructural evolution and mechanical properties of an ultrahigh-strength Al-Zn-Mg-Cu alloy via powder metallurgy and hot extrusion [J]. *Journal of Central South University*, 2021, 28(4): 1195–1205. DOI: 10.1007/s11771-021-4669-y.
- [4] JIA Qing-bo, ROMETSCH P, KÜRNSTEINER P, et al. Selective laser melting of a high strength AlMnSc alloy: Alloy design and strengthening mechanisms [J]. *Acta Materialia*, 2019, 171: 108–118. DOI: 10.1016/j.actamat.2019.04.014.
- [5] ZHA Min, YU Zhi-yuan, QIAN Feng, et al. Achieving dispersed fine soft Bi particles and grain refinement in a hypermonotectic Al-Bi alloy by severe plastic deformation and annealing [J]. *Scripta Materialia*, 2018, 155: 124–128. DOI: 10.1016/j.scriptamat.2018.06.029.
- [6] YANG Xiao-kun, XIONG Bai-qing, LI Xi-wu, et al. Effect of Li addition on mechanical properties and ageing precipitation behavior of extruded Al-3.0Mg-0.5Si alloy [J]. *Journal of Central South University*, 2021, 28(9): 2636–2646. DOI: 10.1007/s11771-021-4798-3.
- [7] XIA Peng, LIU Zhi-yi, BAI Song, et al. Enhanced fatigue crack propagation resistance in a superhigh strength Al-Zn-Mg-Cu alloy by modifying RRA treatment [J]. *Materials Characterization*, 2016, 118: 438–445. DOI: 10.1016/j.matchar.2016.06.023.
- [8] POURNAZARI S, DEEN K M, MAIJER D M, et al. Effect of retrogression and re-ageing (RRA) heat treatment on the corrosion behavior of B206 aluminum-copper casting alloy [J]. *Materials and Corrosion*, 2018, 69(8): 998–1015. DOI: 10.1002/maco.201709925.
- [9] MAYÉN J, ABÚNDEZ A, PORCAYO-CALDERÓN J, et al. Part I: Design and development of new sustainable coatings applied on aluminium 6061 alloy-RRA heat treated for engineering applications [J]. *Surface and Coatings Technology*, 2017, 328: 488–498. DOI: 10.1016/j.surfcoat.2017.09.012.
- [10] MAYÉN J, ABÚNDEZ A, PEREYRA I, et al. Correlation between mechanical properties and corrosion behavior of an Al6061 alloy coated by 5% CH₃COOH pressurized steam

- and RRA heat treated [J]. *Surface and Coatings Technology*, 2017, 309: 344–354. DOI: 10.1016/j.surfcoat.2016.11.053.
- [11] SU R M, QU Y D, LI R D, et al. Influence of RRA treatment on the microstructure and stress corrosion cracking behavior of the spray-formed 7075 alloy [J]. *Materials Science*, 2015, 51(3): 372–380. DOI: 10.1007/s11003-015-9851-7.
- [12] CHANG C S T, WIELER I, WANDERKA N, et al. Positive effect of natural pre-ageing on precipitation hardening in Al-0.44 at% Mg-0.38 at% Si alloy [J]. *Ultramicroscopy*, 2009, 109(5): 585–592. DOI: 10.1016/j.ultramic.2008.12.002.
- [13] ABÚNDEZ A, PEREYRA I, CAMPILLO B, et al. Improvement of ultimate tensile strength by artificial ageing and retrogression treatment of aluminium alloy 6061 [J]. *Materials Science and Engineering A*, 2016, 668: 201–207. DOI: 10.1016/j.msea.2016.05.062.
- [14] ENGLER O, MARIOARA C D, ARUGA Y, et al. Effect of natural ageing or pre-ageing on the evolution of precipitate structure and strength during age hardening of Al-Mg-Si alloy AA 6016 [J]. *Materials Science and Engineering A*, 2019, 759: 520–529. DOI: 10.1016/j.msea.2019.05.073.
- [15] YIN De-yan, XIAO Qiao, CHEN Yu-qiang, et al. Effect of natural ageing and pre-straining on the hardening behaviour and microstructural response during artificial ageing of an Al-Mg-Si-Cu alloy [J]. *Materials & Design*, 2016, 95: 329–339. DOI: 10.1016/j.matdes.2016.01.119.
- [16] JIN Shuo-xun, NGAI T, LI Lie-jun, et al. Influence of natural aging and pre-treatment on the precipitation and age-hardening behavior of Al-1.0Mg-0.65Si-0.24Cu alloy [J]. *Journal of Alloys and Compounds*, 2018, 742: 852–859. DOI: 10.1016/j.jallcom.2017.10.005.
- [17] GONG Wen-yuan, XIE Meng-jing, ZHANG Ji-shan. Giant bake hardening response of multi-scale precipitation strengthened Al-Mg-Si-Cu-Zn alloy via pre-aging treatments [J]. *Materials Characterization*, 2021, 181: 111464. DOI: 10.1016/j.matchar.2021.111464.
- [18] BIROL Y. Pre-aging to improve bake hardening in a twin-roll cast Al-Mg-Si alloy [J]. *Materials Science and Engineering A*, 2005, 391(1, 2): 175–180. DOI: 10.1016/j.msea.2004.08.069.
- [19] DING Li-peng, HE Yang, WEN Zhang, et al. Optimization of the pre-aging treatment for an AA6022 alloy at various temperatures and holding times [J]. *Journal of Alloys and Compounds*, 2015, 647: 238–244. DOI: 10.1016/j.jallcom.2015.05.188.
- [20] GHOSH K S, DAS K, CHATTERJEE U K. Studies of microstructural changes upon retrogression and reaging (RRA) treatment to 8090 Al-Li-Cu-Mg-Zr alloy [J]. *Materials Science and Technology*, 2004, 20(7): 825–834. DOI: 10.1179/026708304225019650.
- [21] WANG Yi-chang, CAO Ling-fei, WU Xiao-dong, et al. Effect of retrogression treatments on microstructure, hardness and corrosion behaviors of aluminum alloy 7085 [J]. *Journal of Alloys and Compounds*, 2020, 814: 152264. DOI: 10.1016/j.jallcom.2019.152264.
- [22] FENG D, ZHANG X M, LIU S D, et al. The effect of pre-ageing temperature and retrogression heating rate on the microstructure and properties of AA7055 [J]. *Materials Science and Engineering A*, 2013, 588: 34–42. DOI: 10.1016/j.msea.2013.09.011.
- [23] NANDANA M S, UDAYA BHAT K, MANJUNATHA C M. Effect of retrogression heat treatment time on microstructure and mechanical properties of AA7010 [J]. *Journal of Materials Engineering and Performance*, 2018, 27(4): 1628–1634. DOI: 10.1007/s11665-018-3268-z.
- [24] ÖZER G, KARAASLAN A. Effect of RRA heat treatment on corrosion and mechanical properties of AA7075 [J]. *Materials and Corrosion*, 2019, 70(11): 2064–2072. DOI: 10.1002/maco.201910955.
- [25] WANG Yi-chang, CAO Ling-fei, WU Xiao-dong, et al. Effect of retrogression treatments on microstructure, hardness and corrosion behaviors of aluminum alloy 7085 [J]. *Journal of Alloys and Compounds*, 2020, 814: 152264. DOI: 10.1016/j.jallcom.2019.152264.
- [26] ÖZER G, KISASÖZ A, KARAASLAN A. Investigation of the relationship between intergranular corrosion and retrogression and reaging in the AA6063 [J]. *Materials and Corrosion*, 2019, 70(12): 2256–2265. DOI: 10.1002/maco.201911100.
- [27] REIS B P, LOPES M M, GARCIA A, et al. The correlation of microstructure features, dry sliding wear behavior, hardness and tensile properties of Al-2wt%Mg-Zn alloys [J]. *Journal of Alloys and Compounds*, 2018, 764: 267–278. DOI: 10.1016/j.jallcom.2018.06.075.
- [28] ASHRAFIZADEH S M, EIVANI A R. Correlative evolution of microstructure, particle dissolution, hardness and strength of ultrafine grained AA6063 alloy during annealing [J]. *Materials Science and Engineering A*, 2015, 644: 284–296. DOI: 10.1016/j.msea.2015.06.074.
- [29] GRONG Ø. Metallurgical modelling of welding [J]. *Materials Characterization*, 1995, 34(4): 289. DOI: 10.1016/1044-5803(95)80084-0.
- [30] TIRYAKIOĞLU M, ROBINSON J S, SALAZAR-GUAPURICHE M A, et al. Hardness-strength relationships in the aluminum alloy 7010 [J]. *Materials Science and Engineering A*, 2015, 631: 196–200. DOI: 10.1016/j.msea.2015.02.049.
- [31] DUNSTAN D J, BUSHBY A J. Grain size dependence of the strength of metals: The Hall-Petch effect does not scale as the inverse square root of grain size [J]. *International Journal of Plasticity*, 2014, 53: 56–65. DOI: 10.1016/j.ijplas.2013.07.004.
- [32] LIU Hong, ZHAO Gang, LIU Chun-ming, et al. Effect of Mn addition on microstructures and properties of Al-Mg-Si-Cu system alloys for automotive body sheets [J]. *Journal of Northeastern University*, 2005, 26(4): 245–248. (in Chinese)
- [33] MAISONNETTE D, SUERY M, NELIAS D, et al. Effects of heat treatments on the microstructure and mechanical properties of a 6061 aluminum alloy [J]. *Materials Science and Engineering A*, 2011, 528(6): 2718–2724. DOI: 10.1016/j.msea.2010.12.011.
- [34] SUNDE J K, LU Feng, MARIOARA C D, et al. Linking mechanical properties to precipitate microstructure in three Al-Mg-Si(-Cu) alloys [J]. *Materials Science and Engineering A*, 2021, 807: 140862. DOI: 10.1016/j.msea.2021.140862.
- [35] NINIVE P H, STRANDLIE A, GULBRANDSEN-DAHL S, et al. Detailed atomistic insight into the β'' phase in Al-Mg-Si alloys [J]. *Acta Materialia*, 2014, 69: 126–134. DOI: 10.1016/j.actamat.2014.01.052.

- [36] VISSERS R, VAN HUIS M A, JANSEN J, et al. The crystal structure of the β' phase in Al-Mg-Si alloys [J]. *Acta Materialia*, 2007, 55(11): 3815 – 3823. DOI: 10.1016/j.actamat.2007.02.032.
- [37] CAO Ling-yong, GUO Ming-xing, CUI Hua, et al. Study on the kinetics of phase transformation $\beta \rightarrow \alpha$ in the homogeneous heat treatment of Al-Mg-Si series alloys [J]. *Acta Metallurgica Sinica*, 2013, 49(4): 428. DOI: 10.3724/sp.j.1037.2012.00608.
- [38] WANG Xiao-na, HAN Li-zhan, GU Jian-feng. Aging precipitation kinetics and strengthening models for aluminum alloys [J]. *The Chinese Journal of Nonferrous Metals*, 2013, 23(10): 2754 – 2768. DOI: 10.19476/j.ysxb.1004.0609.2013.10.005.(in Chinese)
- [39] MYHR O R, GRONG Ø, ANDERSEN S J. Modelling of the age hardening behaviour of Al-Mg-Si alloys [J]. *Acta Materialia*, 2001, 49(1): 65 – 75. DOI: 10.1016/S1359-6454(00)00301-3.

(Edited by HE Yun-bin)

中文导读

双级时效对 6005 铝合金性能的影响与预测模型的建立

摘要：本文对 6005 挤压铝合金进行双级时效热处理，研究 6005 铝合金在不同时效制度下的组织演变规律和力学性能，建立了预时效制度对 6005 铝合金力学性能的预测模型。研究表明，在较高的预时效温度和较短的预时效时间状态下，6005 铝合金的性能优于 T6 态。TEM 观察结果表明，在 160 °C 和 200 °C 预时效状态下，合金存在较高的位错密度和析出相密度，与模型预测结果吻合。

关键词：铝合金；热处理；预测模型；力学性能；强化机制